Supplementary Information

1,2-Dihalodigermenes Bearing Bulky Rind Groups: Synthesis, Characterization, and Conversion to Halogermylenoids

Naoki Hayakawa,[a] Tomohiro Sugahara,[b] Yasuyuki Numata,[a] Hotaka Kawaai,[a] Kenta Yamatani,[a] Shogo Nishimura,[a] Shun Goda,[a] Yuko Suzuki,[b] Tomoharu Tanikawa,[a] Hidetaka Nakai,[a] Daisuke Hashizume,[c] Takahiro Sasamori,*[bd] Norihiro Tokitoh[b] and Tsukasa Matsuo*[a]

[a]*Department of Applied Chemistry, Faculty of Science and Engineering, Kindai University 3-4-1 Kowakae, Higashi-Osaka, Osaka 577-8502, Japan.*
[b]*Institute for Chemical Research, Kyoto University, Gokasho, Uji, Kyoto 611-0011, Japan.*
[c]*Materials Characterization Support Unit, RIKEN Center for Emergent Matter Science, 2-1 Hirosawa, Wako, Saitama 351-0198, Japan.*
[d]*Graduate School of Natural Sciences, Nagoya City University Yamanohata 1, Mizuho-cho, Mizuho-ku, Nagoya, Aichi 467-8501, Japan.*

E-mail: t-matsuo@apch.kindai.riken.jp, sasamori@nsc.nagoya-cu.ac.jp

(submitted to Dalton Transactions)

Contents

1. NMR spectra

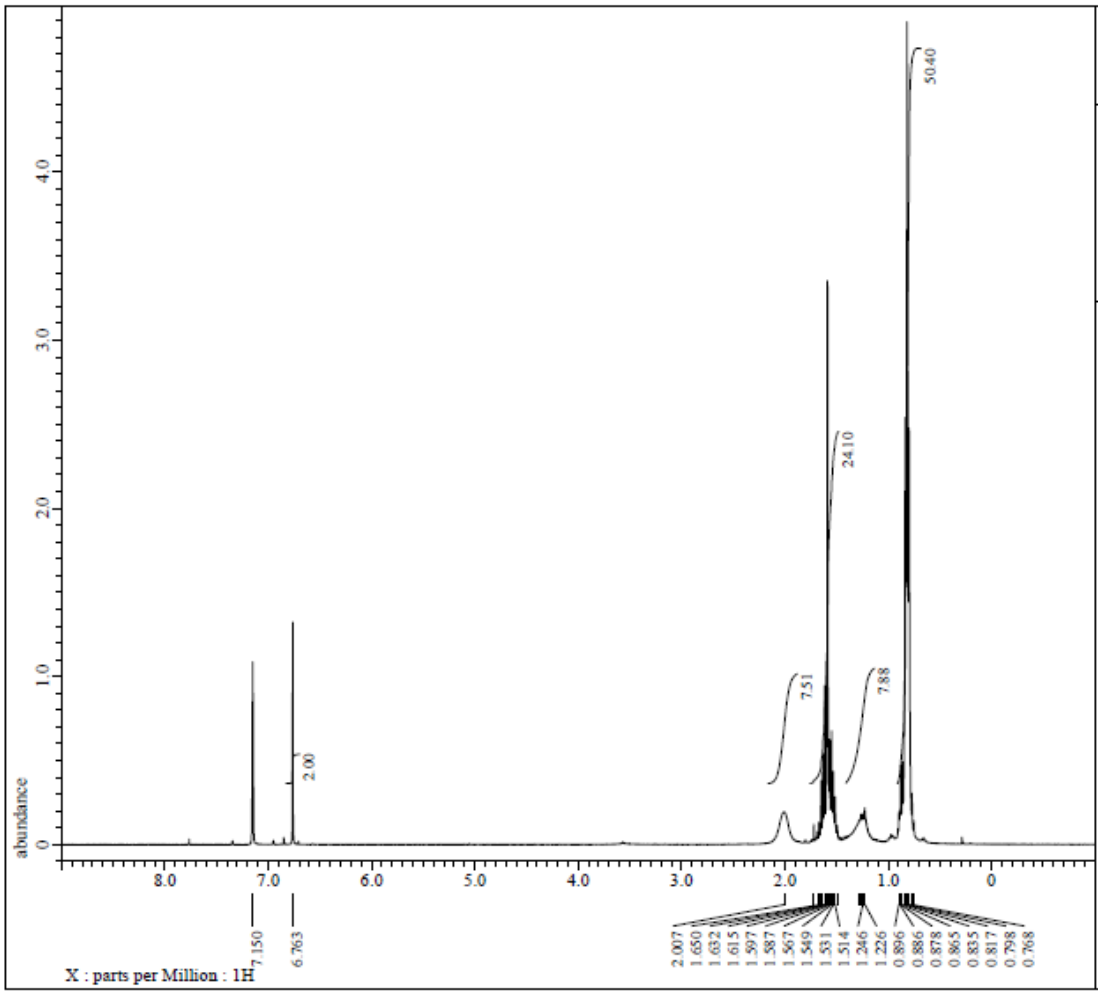

Fig. S1 ^{1}H NMR spectrum of **1** in C_6D_6 at 25 °C.

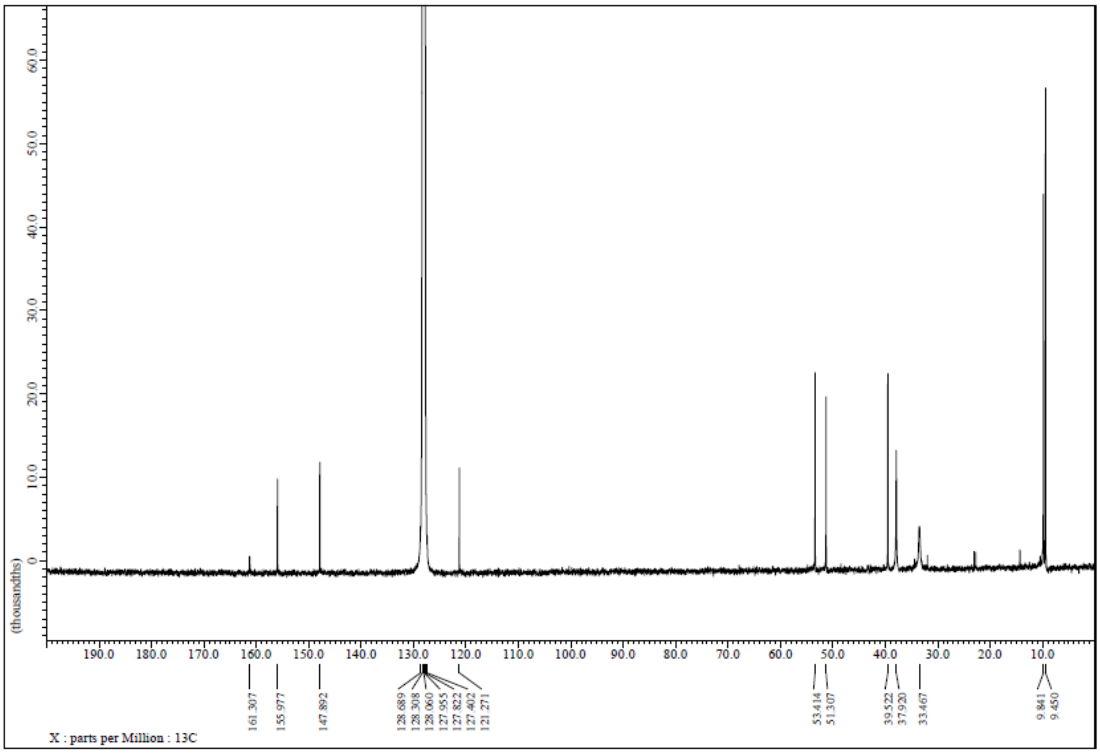

Fig. S2 ^{13}C NMR spectrum of **1** in C_6D_6 at 25 °C.

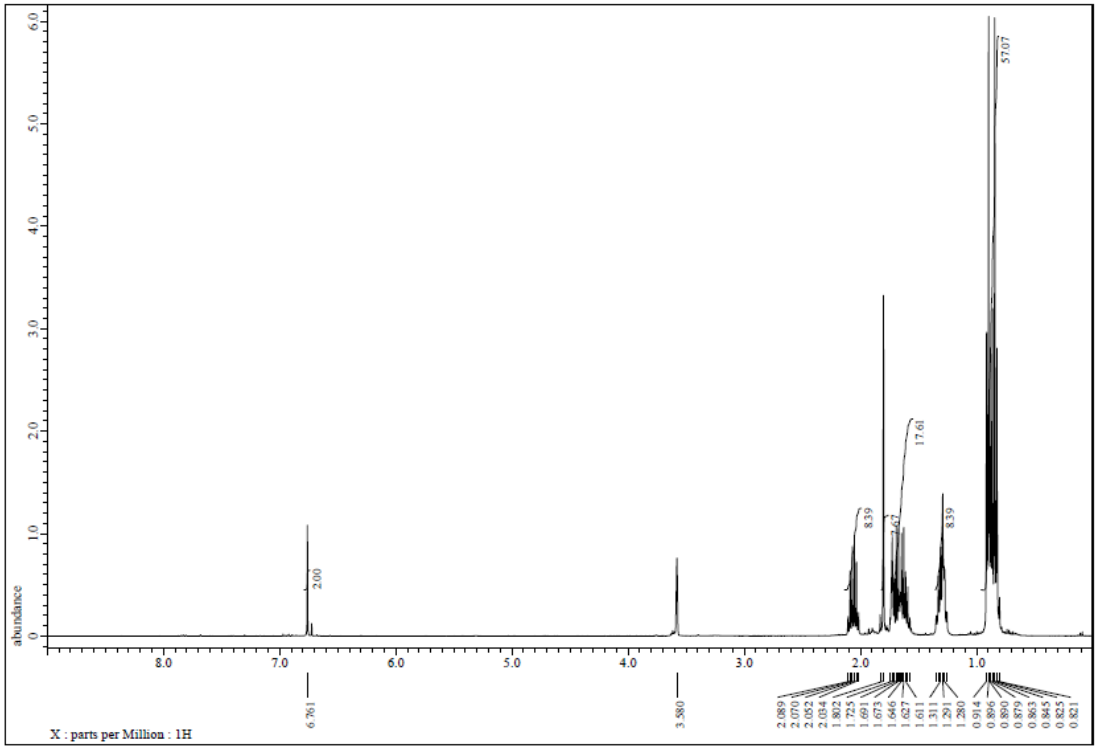

Fig. S3 ^{1}H NMR spectrum of **1** in THF-d_8 at 25 °C.

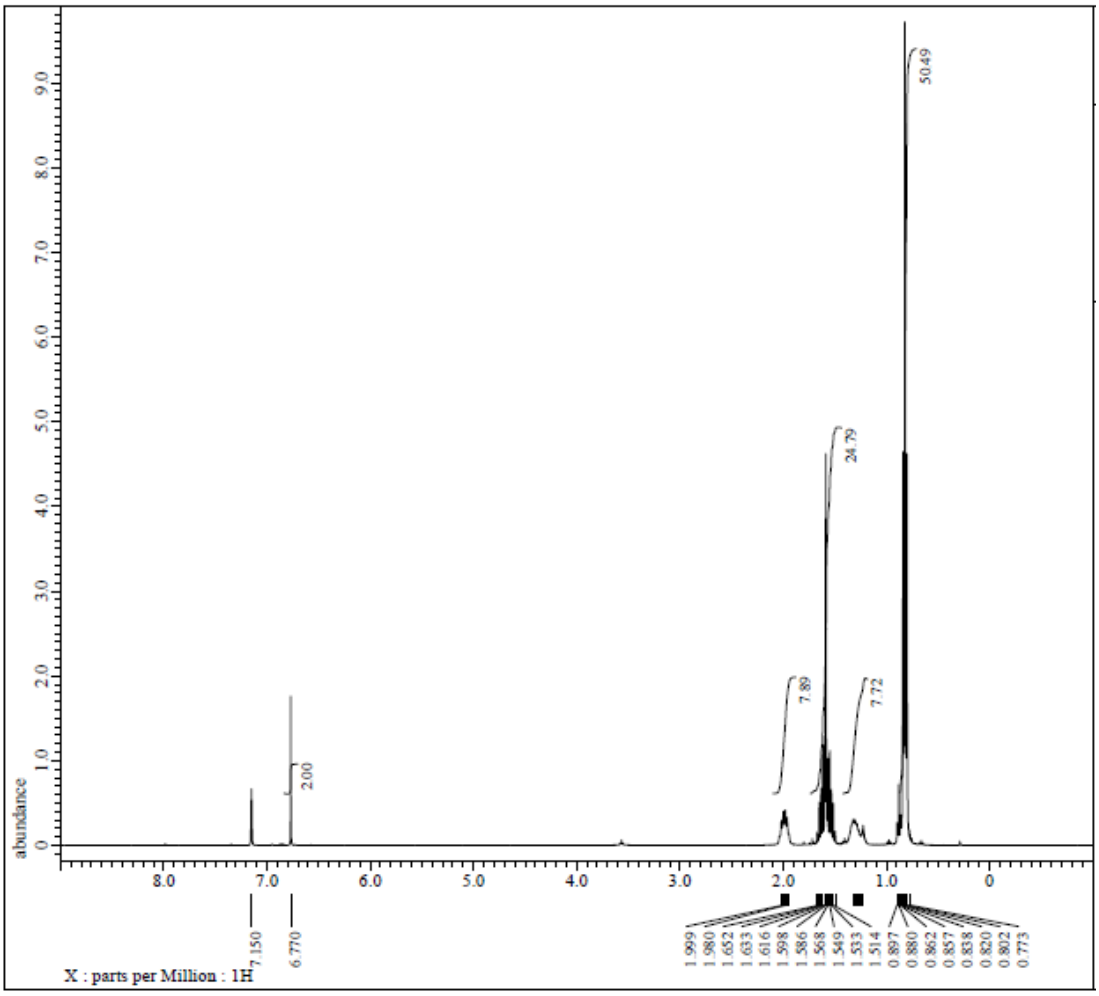

Fig. S4 ^{1}H NMR spectrum of **2** in C_6D_6 at 25 °C.

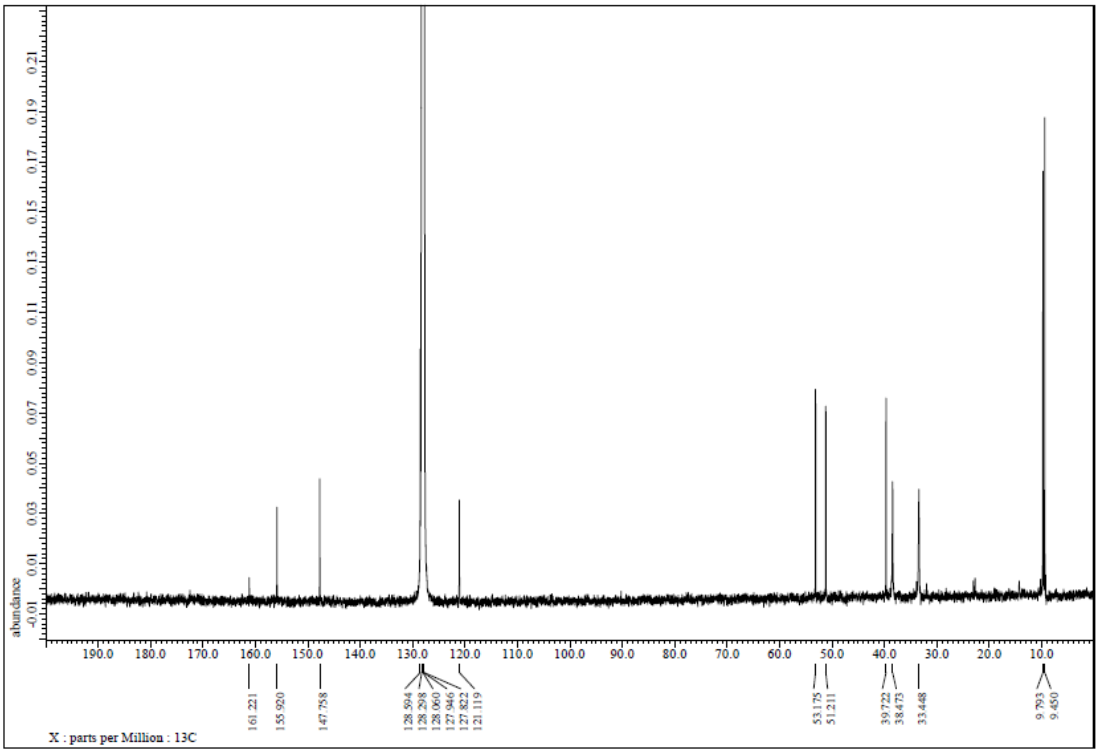

Fig. S5 ^{13}C NMR spectrum of **2** in C_6D_6 at 25 °C.

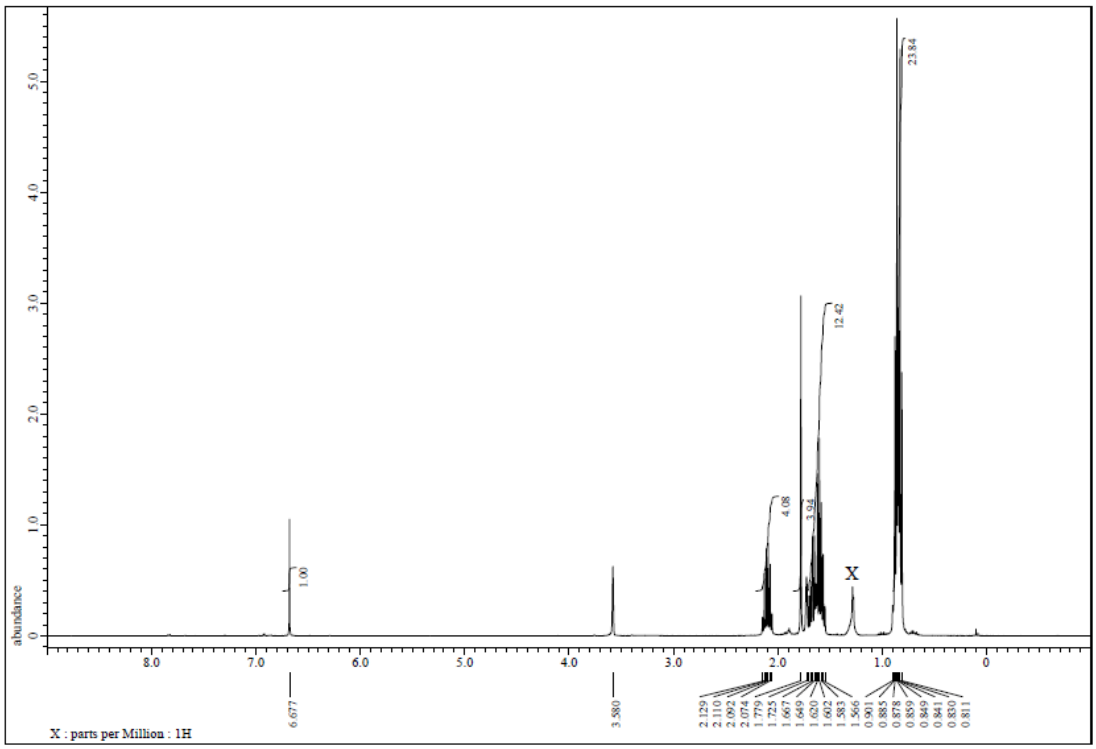

Fig. S6 ^{1}H NMR spectrum of **5** in THF-d_8 at 25 °C (x = hexane).

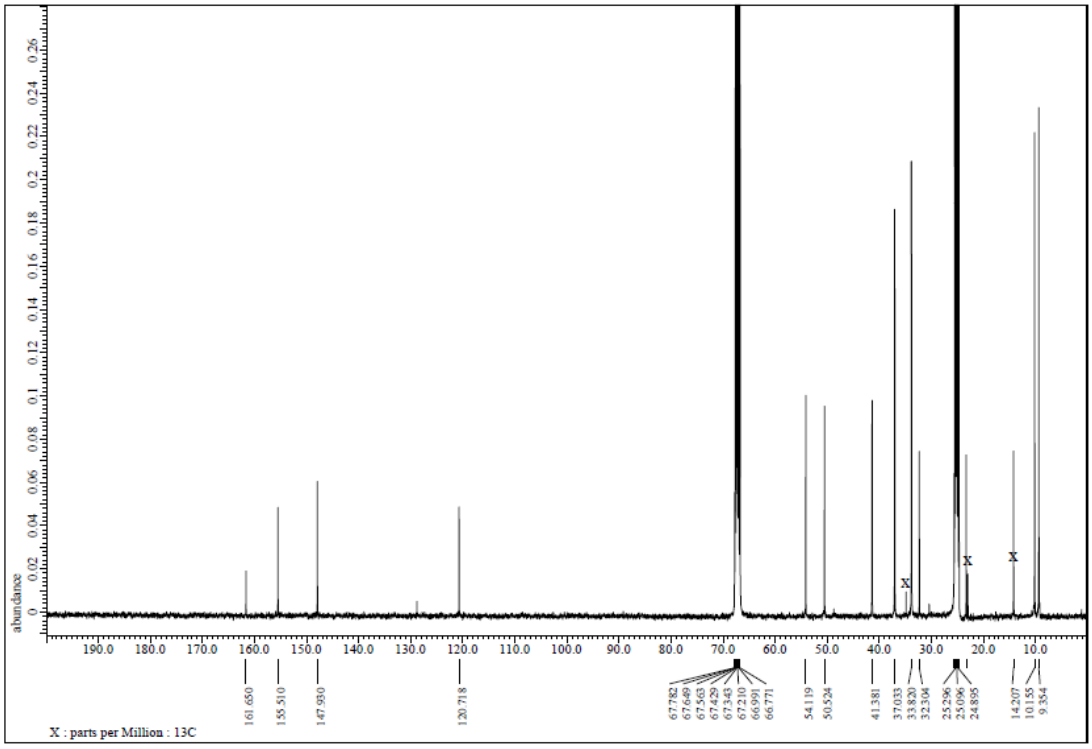

Fig. S7 ^{13}C NMR spectrum of **5** in THF-d_8 at 25 °C (x = hexane).

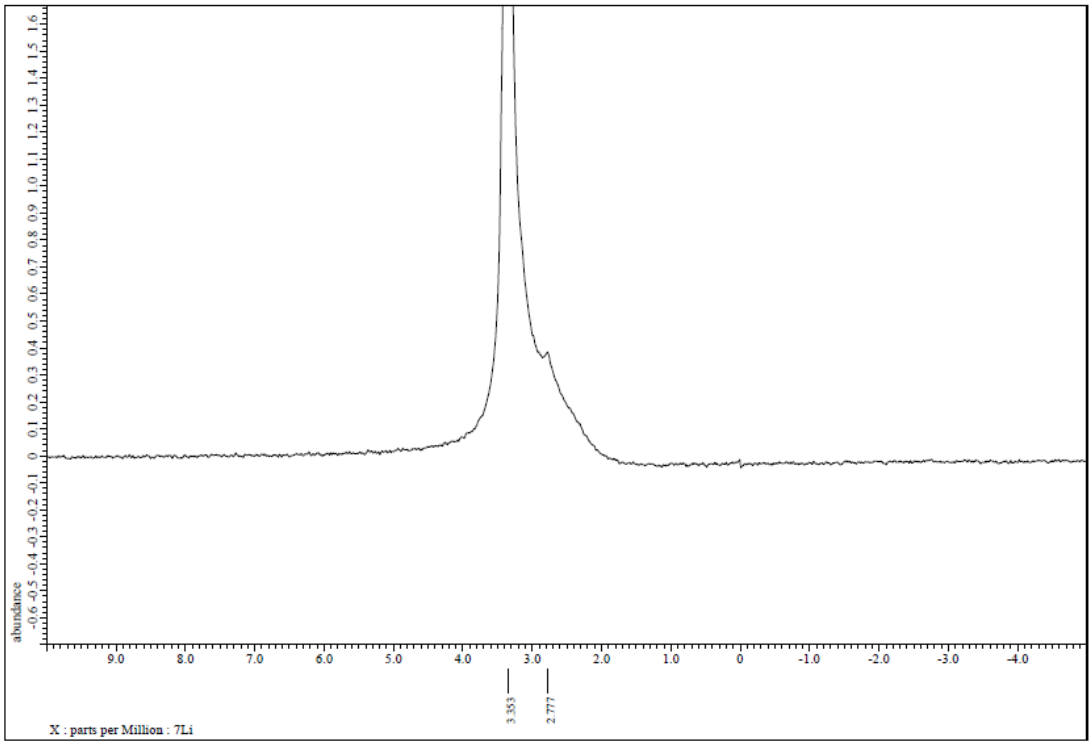

Fig. S8 ^{7}Li NMR spectrum of **5** in THF-d_8 at 25 °C.

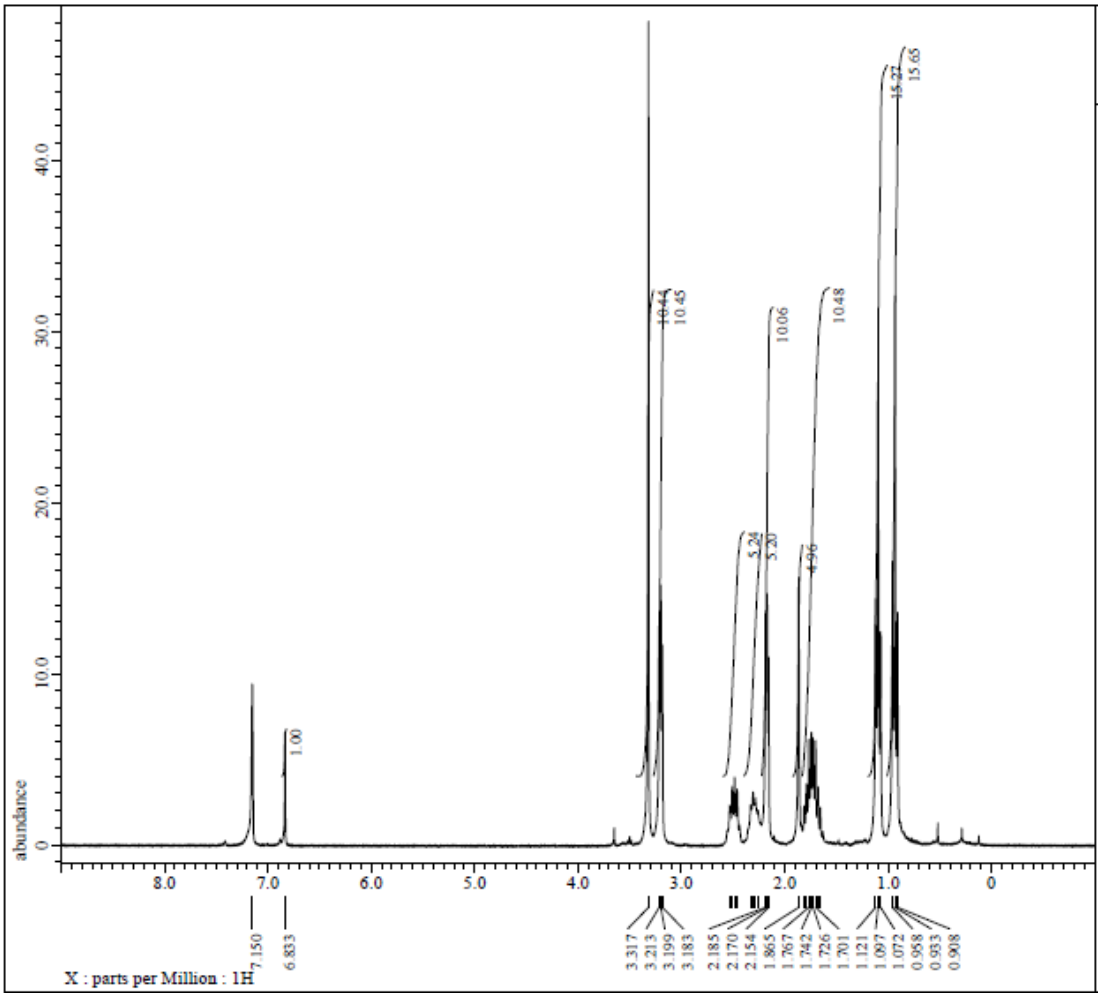

Fig. S9 ^{1}H NMR spectrum of **6** in C_6D_6 at 25 °C.

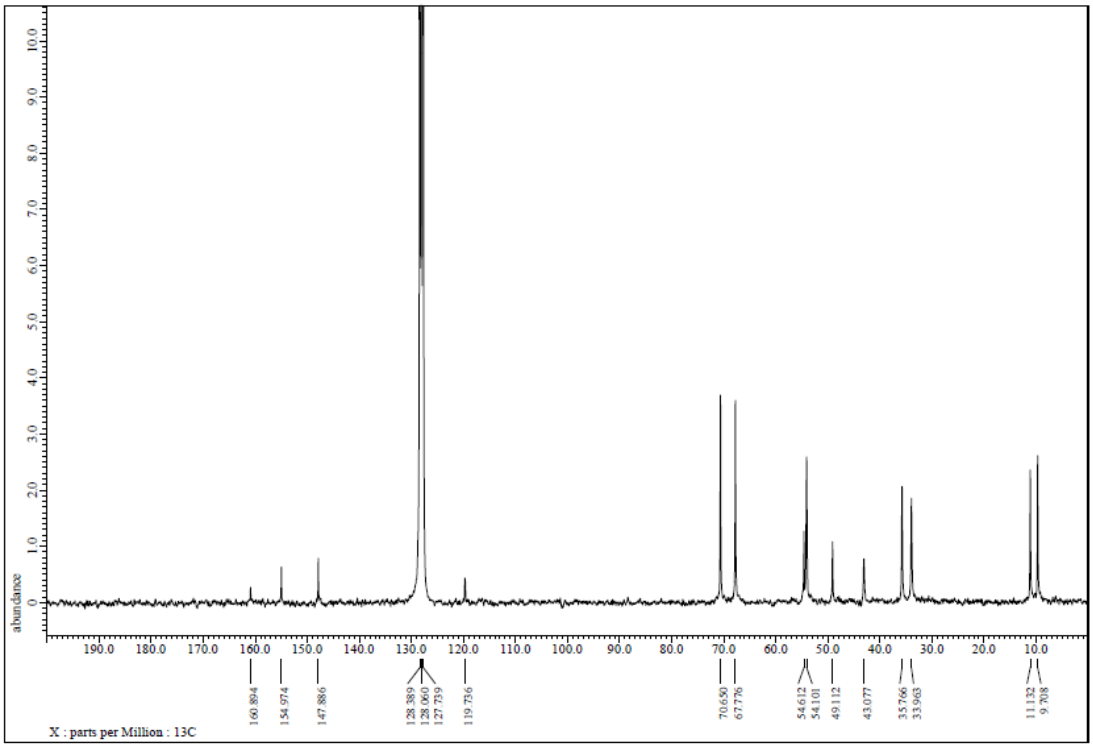

Fig. S10 ^{13}C NMR spectrum of **6** in C_6D_6 at 25 °C.

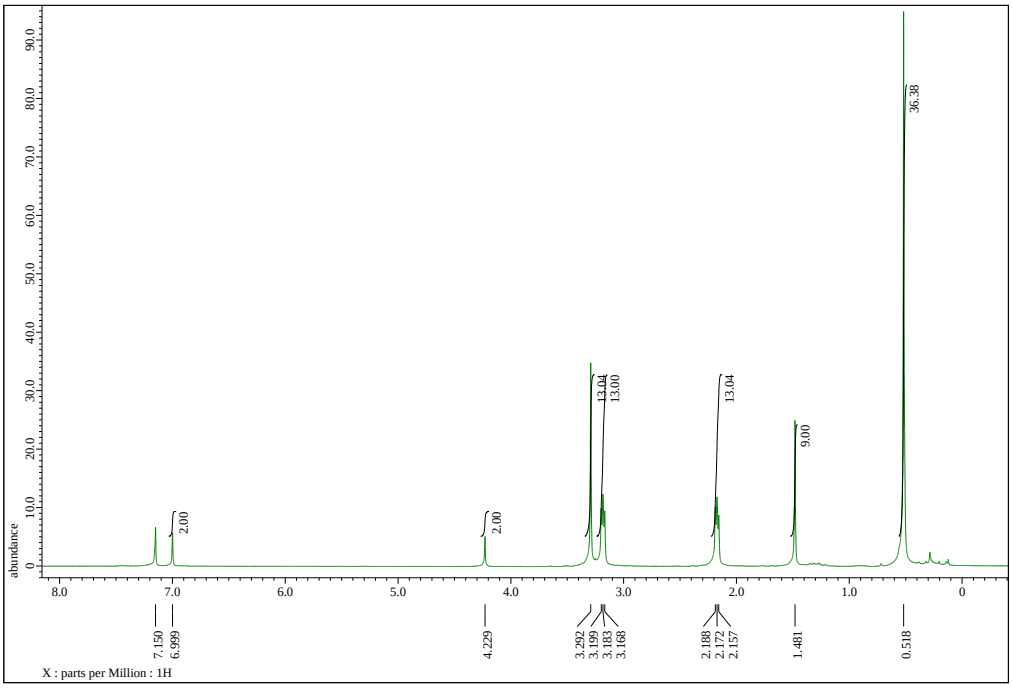

Fig. S11 ^{1}H NMR spectrum of **7** in C_6D_6 at 25 °C.

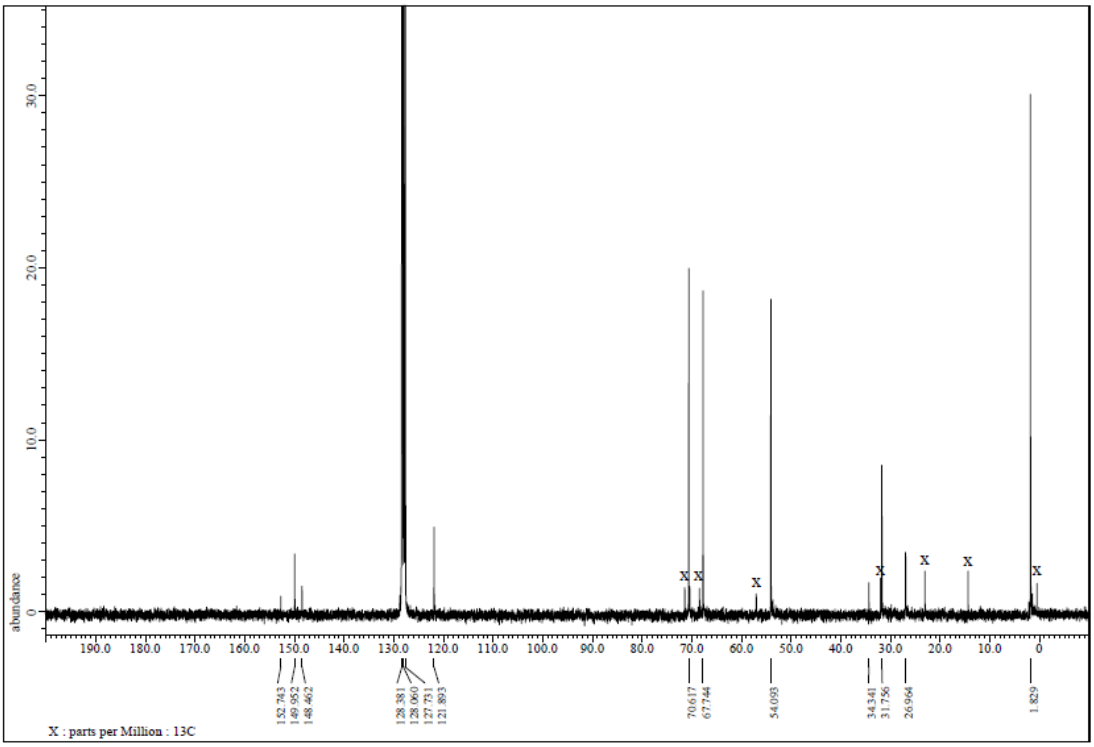

Fig. S12 ^{13}C NMR spectrum of **7** in C_6D_6 at 25 °C (x = impurity).

2. UV-Visible Measurements

The UV-visible spectra were obtained using a Shimadzu UV-1700 pharmaSpec UV-Vis spectrophotometer with S-1700 Thermoelectric Single Cell Holder for **1** (Fig. S13) and **6** (Fig. S17), and a Shimadzu UV-3101(PC)S spectrometer for **2** (Fig. S13). Dry toluene and THF (purchased from Kanto Chemical Co., Inc.) were used for the sample solution. A 1 cm square quartz cell was used for the measurements. The variable-temperature UV-vis spectra of **1** were recorded at 10 °C, 30 °C, 50 °C, and 70 °C for toluene solution (3.4×10^{-4} M) (Fig. S14) and at 25 °C, 40 °C, and 55 °C for THF solution (7.6×10^{-4} M) (Fig. 15). The variable-temperature UV-vis spectra of the mixture of **1** ($[\mathbf{1}]_0$ = ca. 3.3×10^{-4} M) and LiBr ([LiBr] = ca. 3.7×10^{-2} M) in THF were recorded at 25 °C, 40 °C, and 55 °C (Fig. S16). Absorption spectra in a microcrystalline powder film were measured by using a Leica DMLP polarizing microscope connected with a Hamamatsu PMA-11 photodetector (Fig. S18).

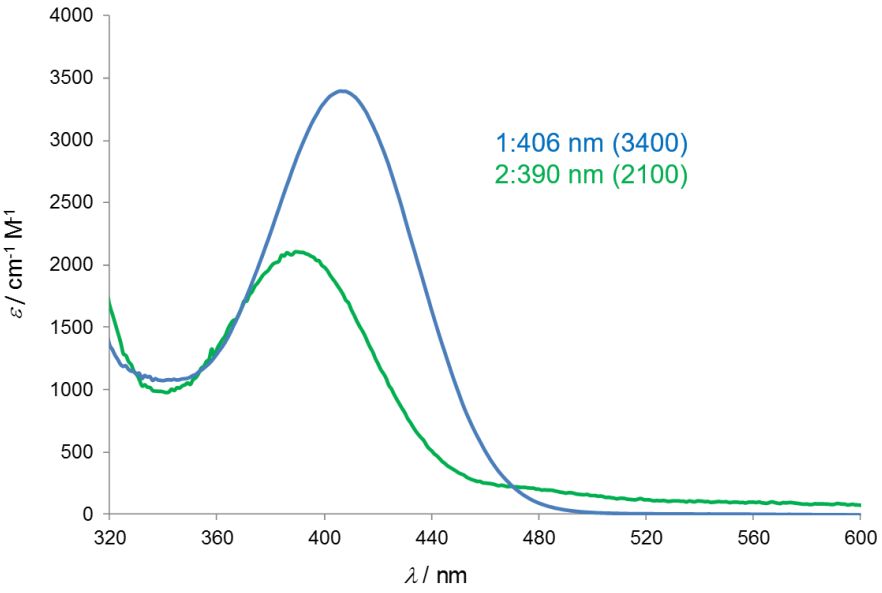

Fig. S13 UV-vis spectra of **1** and **2** in toluene at 25 °C.

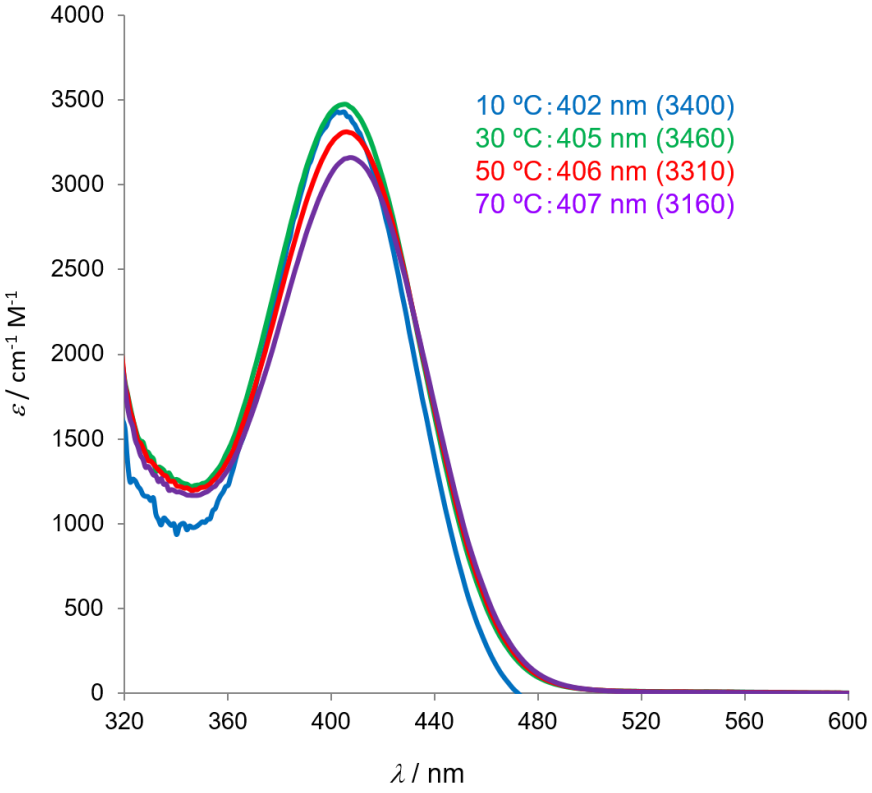

Fig. S14 Variable-temperature UV-vis spectra of **1** in toluene (3.4×10^{-4} M).

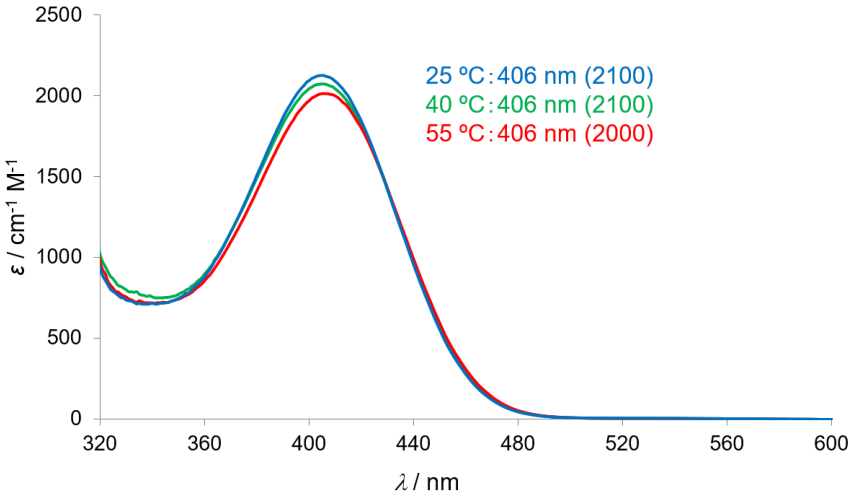

Fig. S15 Variable-temperature UV-vis spectra of **1** in THF (7.6×10^{-4} M).

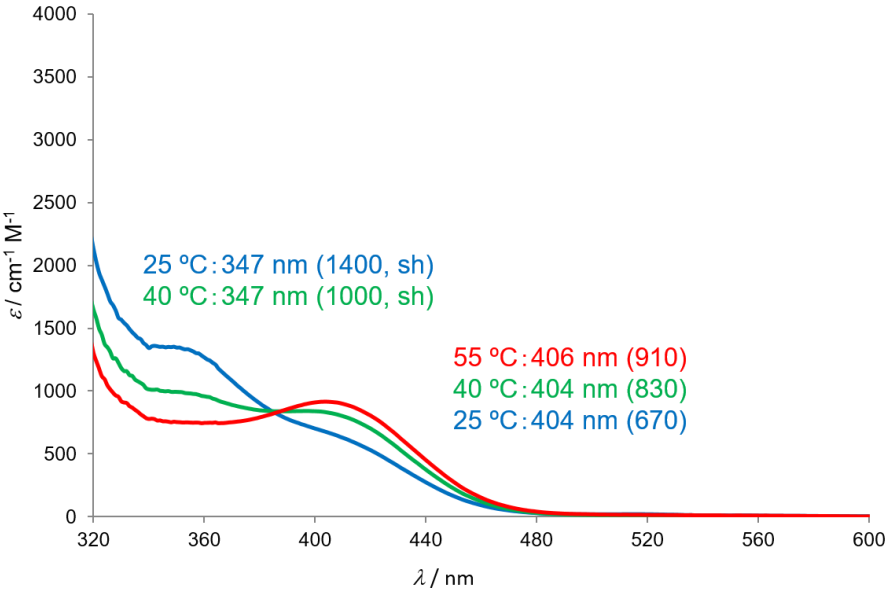

Fig. S16 Variable-temperature UV-vis spectra of **1** with LiBr in THF (3.3×10^{-4} M).

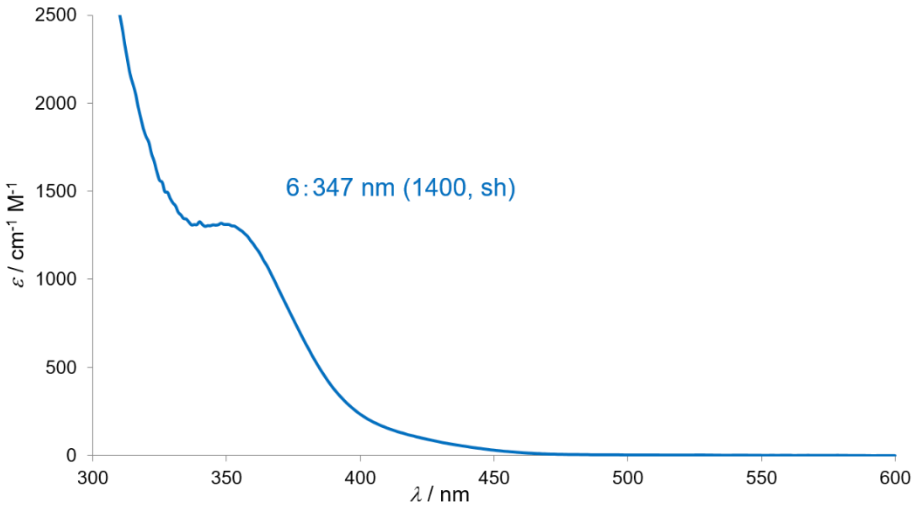

Fig. S17 UV-vis spectrum of **6** in THF (3.7×10^{-4} M).

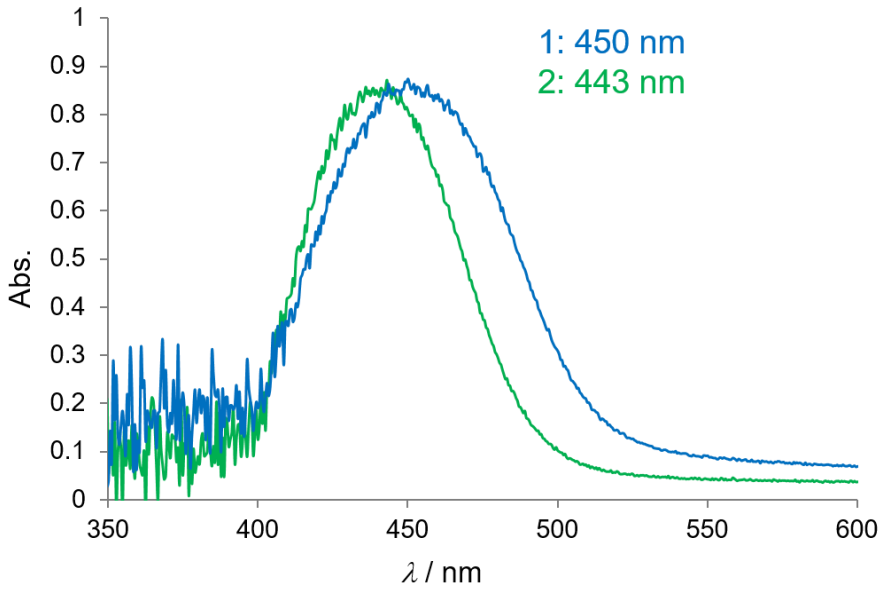

Fig. S18 UV-vis spectra of **1** and **2** in a microcrystalline powder film.

3. X-Ray Crystallographic Analysis

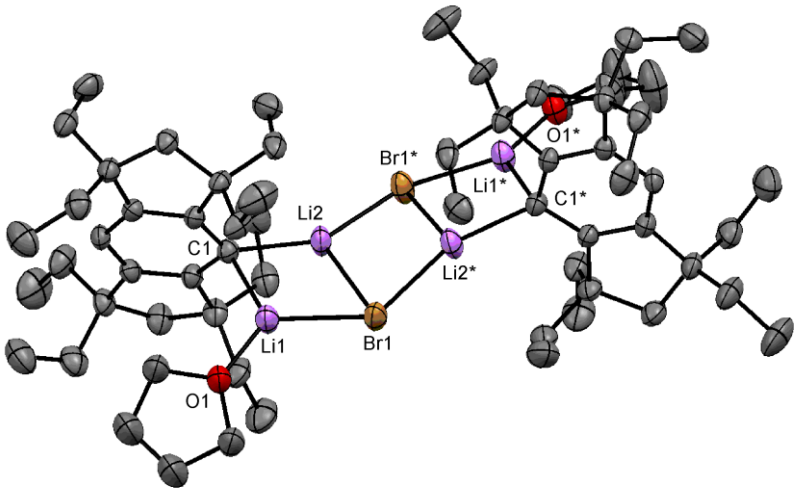

Fig. S19 Molecular structure of $[(Eind)Li(THF)(LiBr)]_2$ (ORTEP drawing; thermal ellipsoids set at 50% probability). Hydrogen atoms and disordered C and O atoms were omitted for clarity and only selected atoms are labeled. Selected atomic distances (Å), bond angles (°): C1–Li1 = 2.138(7), C1–Li2 = 2.147(7), Br1–Li1 = 2.456(6), Br1–Li2 = 2.558(6), Br1–Li2* = 2.475(6), O1–Li1 = 1.877(7), C1–Li1–Br1 = 111.9(3), C1–Li2–Br1 = 107.8(3), C1–Li2–Br1* = 149.5(3), Br1–Li2–Br1* = 102.7(2), C1–Li1–O1 = 119.3(5), Br1–Li1–O1 = 127.9(5), Li1–C1–Li2 = 76.4(3), Li1–Br1–Li2 = 63.8(2), Li2–Br1–Li2* = 75.3(2), Li1–Br1–Li2* = 136.5(2).

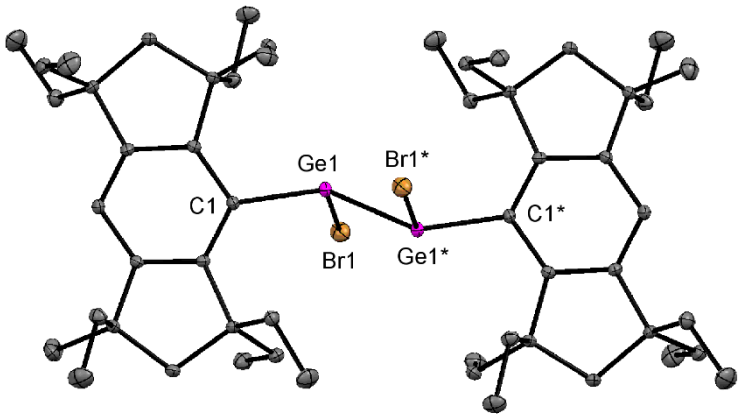

Fig. S20 Molecular structure of **1** (ORTEP drawing; thermal ellipsoids set at 50% probability). Hydrogen atoms were omitted for clarity and only selected atoms are labeled. Selected atomic distances (Å), bond angles (º): Ge1–Ge1* = 2.4145(3), Ge1–Br1 = 2.3622(2), Ge1–C1 = 1.9830(13), C1–Ge1–Br1 = 107.48(4), C1–Ge1–Ge1* = 125.38(4), Br1–Ge1–Ge1* = 104.276(9).

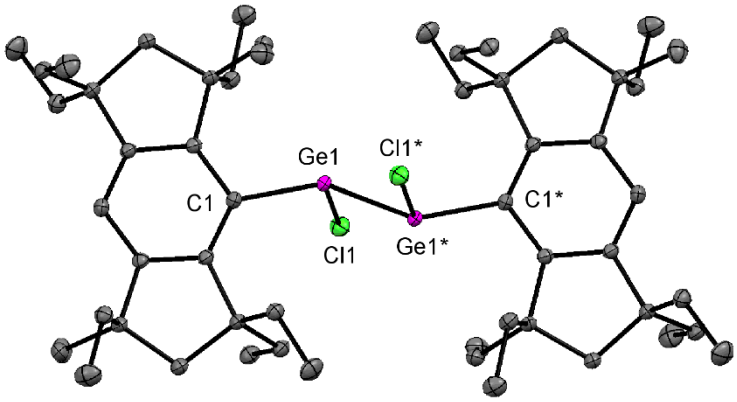

Fig. S21 Molecular structure of **2** (ORTEP drawing; thermal ellipsoids set at 50% probability). Hydrogen atoms and disordered Ge and Cl atoms were omitted for clarity and only selected atoms are labeled. Selected atomic distances (Å), bond angles (º): Ge1–Ge1* = 2.4119(5), Ge1–Cl1 = 2.2124(15), Ge1–C1 = 1.9783(19), C1–Ge1–Cl1 = 106.85(7), C1–Ge1–Ge1* = 125.05(6), Cl1–Ge1–Ge1* = 103.96(5); Ge1B–Ge1B* = 2.363(7), Ge1B–Cl1B = 2.23(3), Ge1B–C1 = 2.070(4), C1–Ge1B–Cl1B = 108.5(7), C1–Ge1B–Ge1B* = 119.8(2), Cl1B–Ge1B–Ge1B* = 105.5(7).

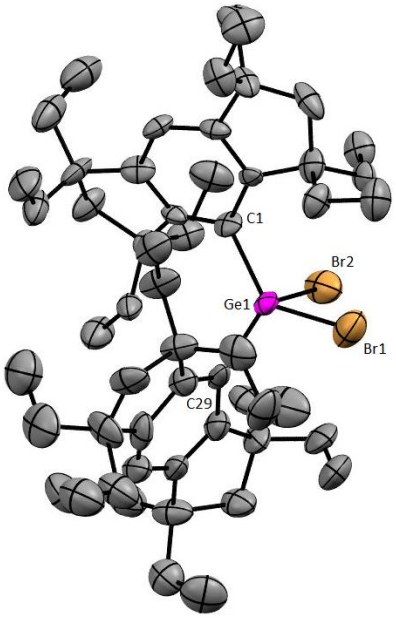

Fig. S22 Molecular structure of $(Eind)_2GeBr_2$ (ORTEP drawing; thermal ellipsoids set at 50% probability). Hydrogen atoms were omitted for clarity and only selected atoms are labeled. Selected atomic distances (Å), bond angles (º): Ge1–C1 = 2.021(15), Ge1–C29 = 2.022(16), Ge1–Br1 = 2.356(3), Ge1–Br2 = 2.363(3), C1–Ge1–C29 = 120.4(6), C1–Ge1–Br1 = 122.7(5), C1–Ge1–Br2 = 98.5(4), C29–Ge1–Br1 = 98.5(4), C29–Ge1–Br2 = 123.8(5), Br1–Ge1–Br2 = 91.15(11).

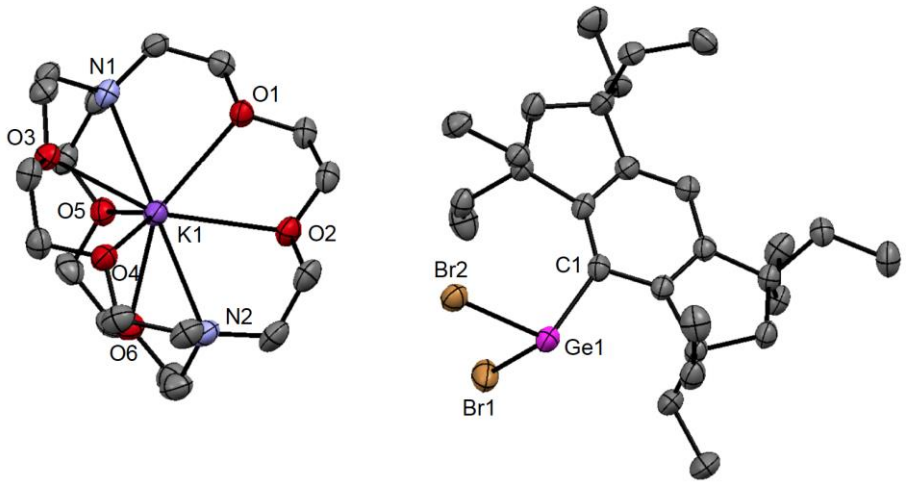

Fig. S23 Molecular structure of **6** (ORTEP drawing; thermal ellipsoids set at 50% probability). Hydrogen atoms and disordered atoms were omitted for clarity and only selected atoms are labeled. Selected atomic distances (Å), bond angles (º): Ge1–Br1 = 2.4780(7), Ge1–Br2 = 2.5562(6), Ge1–C1 = 2.084(4), C1–Ge1–Br1 = 98.57(11), C1–Ge1–Br2 = 113.09(11), Br1–Ge1–Br2 = 96.65(2).

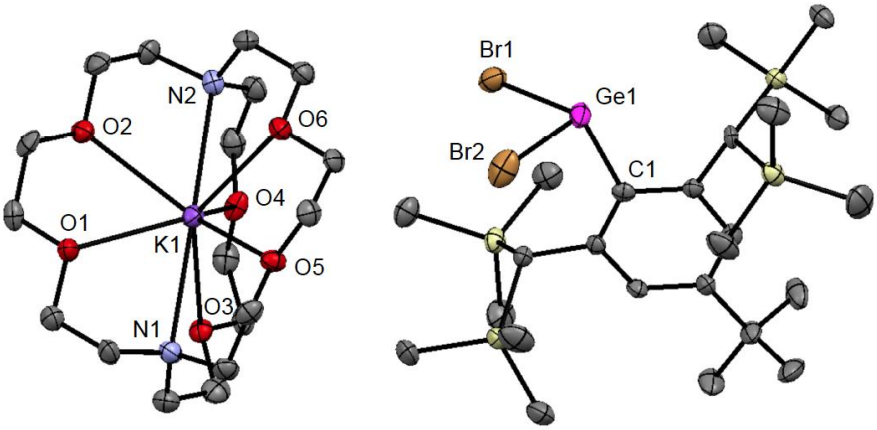

Fig. S24 Molecular structure of **7** (ORTEP drawing; thermal ellipsoids set at 50% probability). Hydrogen atoms and one molecule of benzene were omitted for clarity and only selected atoms are labeled. Selected atomic distances (Å), bond angles (º): Ge1–Br1 = 2.4708(14), Ge1–Br2 = 2.4888(15), Ge1–C1 = 2.044(8), C1–Ge1–Br1 = 103.5(2), C1–Ge1–Br2 = 103.9(2), Br1–Ge1–Br2 = 95.13(5).

Table S1. Crystallographic data for [(Eind)Li(THF)(LiBr)]$_2$, **1**, **2**, (Eind)$_2$GeBr$_2$, **6**, and **7**.

Compound	[(Eind)Li(THF)(LiBr)]$_2$	**1**	**2**	(Eind)$_2$GeBr$_2$	**6**	**7**
Formula	$C_{64}H_{106}Br_2Li_4O_2$	$C_{56}H_{90}Br_2Ge_2$	$C_{56}H_{90}Cl_2Ge_2$	$C_{56}H_{90}Br_2Ge$	$C_{46}H_{81}Br_2GeKN_2O_6$	$C_{45}H_{88}Br_2GeKN_2O_6Si_4$
Molecular weight	1095.06	1068.32	979.35	995.68	1029.63	1137.04
Temperature / °C	–173	–173	–173	–173	–170	–170
λ (Å)	0.71073	0.71073	0.71073	0.71073	0.71073	0.71073
Crystal size / mm^3	0.52 x 0.37 x 0.29	0.11 x 0.07 x 0.06	0.08 x 0.07 x 0.04	0.11 x 0.09 x 0.05	0.08 x 0.07 x 0.04	0.10 x 0.07 x 0.03
Crystal system	Orthorhombic	Triclinic	Triclinic	Monoclinic	Triclinic	Triclinic
Space group	*Pbcn* (#60)	*P*-1 (#2)	*P*-1 (#2)	*Cc* (#9)	*P*-1 (#2)	*P*-1 (#2)
a /Å	19.486(5)	10.43530(14)	10.4792(3)	10.6306(9)	11.2880(9)	11.8021(2)
b /Å	19.226(5)	10.52080(14)	10.5003(2)	26.7797(16)	12.8136(7)	12.4235(3)
c /Å	17.324(4)	12.12440(14)	12.0496(3)	18.0740(14)	18.9434(17)	20.4661(4)
α □°	90	97.1732(10)	97.829(2)	90	104.562(4)	79.3220(10)
β □°	90	93.3651(10)	93.325(2)	101.352(8)	96.164(5)	78.1190(10)
γ □°	90	97.2483(11)	97.830(2)	90	107.936(5)	85.9350(10)
V /Å^3	6490(3)	1306.38(3)	1297.30(6)	5044.7(7)	2471.7(3)	2884.00(10)
Z	4	1	1	4	2	2
μ(Mo-*K*α)/ mm^{-1}	1.287	2.718	1.296	2.226	2.366	2.113
$D_{calcd.}$ / g·cm^{-3}	1.121	1.358	1.254	1.311	1.383	1.309
θ_{max}	27.423	30.000	29.999	26.000	25.999	25.500
Refl./restr./param.	7388/23/337	7611/0/279	7495/18/292	9587/97/548	9641/0/566	10639/0/565
Completeness	99.8	99.9	99.0	99.6	99.3	99.3
GOF	1.139	1.053	1.158	1.026	1.097	1.200
R_1 (I>2σ(I))	0.762	0.0234	0.0428	0.1165	0.0506	0.0872
wR_2 (I>2σ(I))	0.1532	0.0616	0.0980	0.2987	0.1184	0.2161
R_1 (all data)	0.1065	0.0276	0.0515	0.1382	0.0697	0.0943
wR_2 (all data)	0.1696	0.0631	0.1003	0.3214	0.1323	0.2200
Largest diff. peak and hole /e·Å^{-3}	0.537, –0.401	0.949, –0.514	0.953, –0.619	1.726, –1.265	1.303, –0.610	1.708, –1.102
CCDC number	1543443	1542495	1542496	1543095	1543096	1542499